

Measurement of the Relative Branching Fractions of $\bar{B} \rightarrow D/D^*/D^{**}\ell^-\bar{\nu}_\ell$ Decays in Events with a Fully Reconstructed B Meson

B. Aubert,¹ M. Bona,¹ D. Boutigny,¹ Y. Karyotakis,¹ J. P. Lees,¹ V. Poireau,¹ X. Prudent,¹ V. Tisserand,¹
A. Zghiche,¹ J. Garra Tico,² E. Grauges,² L. Lopez,³ A. Palano,³ G. Eigen,⁴ I. Ofte,⁴ B. Stugu,⁴ L. Sun,⁴
G. S. Abrams,⁵ M. Battaglia,⁵ D. N. Brown,⁵ J. Button-Shafer,⁵ R. N. Cahn,⁵ Y. Groyzman,⁵ R. G. Jacobsen,⁵
J. A. Kadyk,⁵ L. T. Kerth,⁵ Yu. G. Kolomensky,⁵ G. Kukartsev,⁵ D. Lopes Pegna,⁵ G. Lynch,⁵ L. M. Mir,⁵
T. J. Orimoto,⁵ M. Pripstein,⁵ N. A. Roe,⁵ M. T. Ronan,^{5,*} K. Tackmann,⁵ W. A. Wenzel,⁵ P. del Amo Sanchez,⁶
C. M. Hawkes,⁶ A. T. Watson,⁶ T. Held,⁷ H. Koch,⁷ B. Lewandowski,⁷ M. Pelizaeus,⁷ T. Schroeder,⁷
M. Steinke,⁷ W. N. Cottingham,⁸ D. Walker,⁸ D. J. Asgeirsson,⁹ T. Cuhadar-Donszelmann,⁹ B. G. Fulsom,⁹
C. Hearty,⁹ N. S. Knecht,⁹ T. S. Mattison,⁹ J. A. McKenna,⁹ A. Khan,¹⁰ M. Saleem,¹⁰ L. Teodorescu,¹⁰
V. E. Blinov,¹¹ A. D. Bukin,¹¹ V. P. Druzhinin,¹¹ V. B. Golubev,¹¹ A. P. Onuchin,¹¹ S. I. Serednyakov,¹¹
Yu. I. Skovpen,¹¹ E. P. Solodov,¹¹ K. Yu. Todyshev,¹¹ M. Bondioli,¹² S. Curry,¹² I. Eschrich,¹² D. Kirkby,¹²
A. J. Lankford,¹² P. Lund,¹² M. Mandelkern,¹² E. C. Martin,¹² D. P. Stoker,¹² S. Abachi,¹³ C. Buchanan,¹³
S. D. Foulkes,¹⁴ J. W. Gary,¹⁴ F. Liu,¹⁴ O. Long,¹⁴ B. C. Shen,¹⁴ L. Zhang,¹⁴ H. P. Paar,¹⁵ S. Rahatlou,¹⁵
V. Sharma,¹⁵ J. W. Berryhill,¹⁶ C. Campagnari,¹⁶ A. Cunha,¹⁶ B. Dahmes,¹⁶ T. M. Hong,¹⁶ D. Kovalskyi,¹⁶
J. D. Richman,¹⁶ T. W. Beck,¹⁷ A. M. Eisner,¹⁷ C. J. Flacco,¹⁷ C. A. Heusch,¹⁷ J. Kroseberg,¹⁷ W. S. Lockman,¹⁷
T. Schalk,¹⁷ B. A. Schumm,¹⁷ A. Seiden,¹⁷ D. C. Williams,¹⁷ M. G. Wilson,¹⁷ L. O. Winstrom,¹⁷ E. Chen,¹⁸
C. H. Cheng,¹⁸ A. Dvoretzki,¹⁸ F. Fang,¹⁸ D. G. Hitlin,¹⁸ I. Narsky,¹⁸ T. Piatenko,¹⁸ F. C. Porter,¹⁸
G. Mancinelli,¹⁹ B. T. Meadows,¹⁹ K. Mishra,¹⁹ M. D. Sokoloff,¹⁹ F. Blanc,²⁰ P. C. Bloom,²⁰ S. Chen,²⁰
W. T. Ford,²⁰ J. F. Hirschauer,²⁰ A. Kreisel,²⁰ M. Nagel,²⁰ U. Nauenberg,²⁰ A. Olivas,²⁰ J. G. Smith,²⁰
K. A. Ulmer,²⁰ S. R. Wagner,²⁰ J. Zhang,²⁰ A. M. Gabareen,²¹ A. Soffer,²¹ W. H. Toki,²¹ R. J. Wilson,²¹
F. Winklmeier,²¹ Q. Zeng,²¹ D. D. Altenburg,²² E. Feltresi,²² A. Hauke,²² H. Jasper,²² J. Merkel,²² A. Petzold,²²
B. Spaan,²² K. Wacker,²² T. Brandt,²³ V. Klose,²³ H. M. Lacker,²³ W. F. Mader,²³ R. Nogowski,²³ J. Schubert,²³
K. R. Schubert,²³ R. Schwierz,²³ J. E. Sundermann,²³ A. Volk,²³ D. Bernard,²⁴ G. R. Bonneaud,²⁴ E. Latour,²⁴
V. Lombardo,²⁴ Ch. Thiebaut,²⁴ M. Verderi,²⁴ P. J. Clark,²⁵ W. Gradl,²⁵ F. Muheim,²⁵ S. Playfer,²⁵
A. I. Robertson,²⁵ Y. Xie,²⁵ M. Andreotti,²⁶ D. Bettoni,²⁶ C. Bozzi,²⁶ R. Calabrese,²⁶ A. Cecchi,²⁶ G. Cibinetto,²⁶
P. Franchini,²⁶ E. Luppi,²⁶ M. Negrini,²⁶ A. Petrella,²⁶ L. Piemontese,²⁶ E. Prencipe,²⁶ V. Santoro,²⁶ F. Anulli,²⁷
R. Baldini-Ferroli,²⁷ A. Calcaterra,²⁷ R. de Sangro,²⁷ G. Finocchiaro,²⁷ S. Pacetti,²⁷ P. Patteri,²⁷ I. M. Peruzzi,^{27,†}
M. Piccolo,²⁷ M. Rama,²⁷ A. Zallo,²⁷ A. Buzzo,²⁸ R. Contri,²⁸ M. Lo Vetere,²⁸ M. M. Macri,²⁸ M. R. Monge,²⁸
S. Passaggio,²⁸ C. Patrignani,²⁸ E. Robutti,²⁸ A. Santroni,²⁸ S. Tosi,²⁸ K. S. Chaisanguanthum,²⁹ M. Morii,²⁹
J. Wu,²⁹ R. S. Dubitzky,³⁰ J. Marks,³⁰ S. Schenk,³⁰ U. Uwer,³⁰ D. J. Bard,³¹ P. D. Dauncey,³¹ R. L. Flack,³¹
J. A. Nash,³¹ M. B. Nikolich,³¹ W. Panduro Vazquez,³¹ P. K. Behera,³² X. Chai,³² M. J. Charles,³² U. Mallik,³²
N. T. Meyer,³² V. Ziegler,³² J. Cochran,³³ H. B. Crawley,³³ L. Dong,³³ V. Eyges,³³ W. T. Meyer,³³ S. Prell,³³
E. I. Rosenberg,³³ A. E. Rubin,³³ A. V. Gritsan,³⁴ Z. J. Guo,³⁴ C. K. Lae,³⁴ A. G. Denig,³⁵ M. Fritsch,³⁵
G. Schott,³⁵ N. Arnaud,³⁶ J. Béquilleux,³⁶ M. Davier,³⁶ G. Grosdidier,³⁶ A. Höcker,³⁶ V. Lepeltier,³⁶
F. Le Diberder,³⁶ A. M. Lutz,³⁶ S. Pruvot,³⁶ S. Rodier,³⁶ P. Roudeau,³⁶ M. H. Schune,³⁶ J. Serrano,³⁶ V. Sordini,³⁶
A. Stocchi,³⁶ W. F. Wang,³⁶ G. Wormser,³⁶ D. J. Lange,³⁷ D. M. Wright,³⁷ C. A. Chavez,³⁸ I. J. Forster,³⁸
J. R. Fry,³⁸ E. Gabathuler,³⁸ R. Gamet,³⁸ D. E. Hutchcroft,³⁸ D. J. Payne,³⁸ K. C. Schofield,³⁸ C. Touramanis,³⁸
A. J. Bevan,³⁹ K. A. George,³⁹ F. Di Lodovico,³⁹ W. Menges,³⁹ R. Sacco,³⁹ G. Cowan,⁴⁰ H. U. Flaecher,⁴⁰
D. A. Hopkins,⁴⁰ P. S. Jackson,⁴⁰ T. R. McMahon,⁴⁰ F. Salvatore,⁴⁰ A. C. Wren,⁴⁰ D. N. Brown,⁴¹ C. L. Davis,⁴¹
J. Allison,⁴² N. R. Barlow,⁴² R. J. Barlow,⁴² Y. M. Chia,⁴² C. L. Edgar,⁴² G. D. Lafferty,⁴² T. J. West,⁴²
J. I. Yi,⁴² J. Anderson,⁴³ C. Chen,⁴³ A. Jawahery,⁴³ D. A. Roberts,⁴³ G. Simi,⁴³ J. M. Tuggle,⁴³ G. Blaylock,⁴⁴
C. Dallapiccola,⁴⁴ S. S. Hertzbach,⁴⁴ X. Li,⁴⁴ T. B. Moore,⁴⁴ E. Salvati,⁴⁴ S. Saremi,⁴⁴ R. Cowan,⁴⁵ P. H. Fisher,⁴⁵
G. Sciolla,⁴⁵ S. J. Sekula,⁴⁵ M. Spitznagel,⁴⁵ F. Taylor,⁴⁵ R. K. Yamamoto,⁴⁵ S. E. Mclachlin,⁴⁶ P. M. Patel,⁴⁶
S. H. Robertson,⁴⁶ A. Lazzaro,⁴⁷ F. Palombo,⁴⁷ J. M. Bauer,⁴⁸ L. Cremaldi,⁴⁸ V. Eschenburg,⁴⁸ R. Godang,⁴⁸
R. Kroeger,⁴⁸ D. A. Sanders,⁴⁸ D. J. Summers,⁴⁸ H. W. Zhao,⁴⁸ S. Brunet,⁴⁹ D. Côté,⁴⁹ M. Simard,⁴⁹ P. Taras,⁴⁹
F. B. Viaud,⁴⁹ H. Nicholson,⁵⁰ G. De Nardo,⁵¹ F. Fabozzi,^{51,‡} L. Lista,⁵¹ D. Monorchio,⁵¹ C. Sciacca,⁵¹
M. A. Baak,⁵² G. Raven,⁵² H. L. Snoek,⁵² C. P. Jessop,⁵³ J. M. LoSecco,⁵³ G. Benelli,⁵⁴ L. A. Corwin,⁵⁴
K. K. Gan,⁵⁴ K. Honscheid,⁵⁴ D. Hufnagel,⁵⁴ H. Kagan,⁵⁴ R. Kass,⁵⁴ J. P. Morris,⁵⁴ A. M. Rahimi,⁵⁴

J. J. Regensburger,⁵⁴ R. Ter-Antonyan,⁵⁴ Q. K. Wong,⁵⁴ N. L. Blount,⁵⁵ J. Brau,⁵⁵ R. Frey,⁵⁵ O. Igonkina,⁵⁵ J. A. Kolb,⁵⁵ M. Lu,⁵⁵ R. Rahmat,⁵⁵ N. B. Sinev,⁵⁵ D. Strom,⁵⁵ J. Strube,⁵⁵ E. Torrence,⁵⁵ N. Gagliardi,⁵⁶ A. Gaz,⁵⁶ M. Margoni,⁵⁶ M. Morandin,⁵⁶ A. Pompili,⁵⁶ M. Posocco,⁵⁶ M. Rotondo,⁵⁶ F. Simonetto,⁵⁶ R. Stroili,⁵⁶ C. Voci,⁵⁶ E. Ben-Haim,⁵⁷ H. Briand,⁵⁷ J. Chauveau,⁵⁷ P. David,⁵⁷ L. Del Buono,⁵⁷ Ch. de la Vaissière,⁵⁷ O. Hamon,⁵⁷ B. L. Hartfiel,⁵⁷ Ph. Leruste,⁵⁷ J. Malclès,⁵⁷ J. Ocariz,⁵⁷ A. Perez,⁵⁷ L. Gladney,⁵⁸ M. Biasini,⁵⁹ R. Covarelli,⁵⁹ E. Manoni,⁵⁹ C. Angelini,⁶⁰ G. Batignani,⁶⁰ S. Bettarini,⁶⁰ G. Calderini,⁶⁰ M. Carpinelli,⁶⁰ R. Cenci,⁶⁰ A. Cervelli,⁶⁰ F. Forti,⁶⁰ M. A. Giorgi,⁶⁰ A. Lusiani,⁶⁰ G. Marchiori,⁶⁰ M. A. Mazur,⁶⁰ M. Morganti,⁶⁰ N. Neri,⁶⁰ E. Paoloni,⁶⁰ G. Rizzo,⁶⁰ J. J. Walsh,⁶⁰ M. Haire,⁶¹ J. Biesiada,⁶² P. Elmer,⁶² Y. P. Lau,⁶² C. Lu,⁶² J. Olsen,⁶² A. J. S. Smith,⁶² A. V. Telnov,⁶² E. Baracchini,⁶³ F. Bellini,⁶³ G. Cavoto,⁶³ A. D’Orazio,⁶³ D. del Re,⁶³ E. Di Marco,⁶³ R. Faccini,⁶³ F. Ferrarotto,⁶³ F. Ferroni,⁶³ M. Gaspero,⁶³ P. D. Jackson,⁶³ L. Li Gioi,⁶³ M. A. Mazzoni,⁶³ S. Morganti,⁶³ G. Piredda,⁶³ F. Polci,⁶³ F. Renga,⁶³ C. Voena,⁶³ M. Ebert,⁶⁴ H. Schröder,⁶⁴ R. Waldi,⁶⁴ T. Adye,⁶⁵ G. Castelli,⁶⁵ B. Franek,⁶⁵ E. O. Olaiya,⁶⁵ S. Ricciardi,⁶⁵ W. Roethel,⁶⁵ F. F. Wilson,⁶⁵ R. Aleksan,⁶⁶ S. Emery,⁶⁶ M. Escalier,⁶⁶ A. Gaidot,⁶⁶ S. F. Ganzhur,⁶⁶ G. Hamel de Monchenault,⁶⁶ W. Kozanecki,⁶⁶ M. Legendre,⁶⁶ G. Vasseur,⁶⁶ Ch. Yèche,⁶⁶ M. Zito,⁶⁶ X. R. Chen,⁶⁷ H. Liu,⁶⁷ W. Park,⁶⁷ M. V. Purohit,⁶⁷ J. R. Wilson,⁶⁷ M. T. Allen,⁶⁸ D. Aston,⁶⁸ R. Bartoldus,⁶⁸ P. Bechtle,⁶⁸ N. Berger,⁶⁸ R. Claus,⁶⁸ J. P. Coleman,⁶⁸ M. R. Convery,⁶⁸ J. C. Dingfelder,⁶⁸ J. Dorfan,⁶⁸ G. P. Dubois-Felsmann,⁶⁸ D. Dujmic,⁶⁸ W. Dunwoodie,⁶⁸ R. C. Field,⁶⁸ T. Glanzman,⁶⁸ S. J. Gowdy,⁶⁸ M. T. Graham,⁶⁸ P. Grenier,⁶⁸ C. Hast,⁶⁸ T. Hryn’ova,⁶⁸ W. R. Innes,⁶⁸ M. H. Kelsey,⁶⁸ H. Kim,⁶⁸ P. Kim,⁶⁸ D. W. G. S. Leith,⁶⁸ S. Li,⁶⁸ S. Luitz,⁶⁸ V. Luth,⁶⁸ H. L. Lynch,⁶⁸ D. B. MacFarlane,⁶⁸ H. Marsiske,⁶⁸ R. Messner,⁶⁸ D. R. Muller,⁶⁸ C. P. O’Grady,⁶⁸ A. Perazzo,⁶⁸ M. Perl,⁶⁸ T. Pulliam,⁶⁸ B. N. Ratcliff,⁶⁸ A. Roodman,⁶⁸ A. A. Salnikov,⁶⁸ R. H. Schindler,⁶⁸ J. Schwiening,⁶⁸ A. Snyder,⁶⁸ J. Stelzer,⁶⁸ D. Su,⁶⁸ M. K. Sullivan,⁶⁸ K. Suzuki,⁶⁸ S. K. Swain,⁶⁸ J. M. Thompson,⁶⁸ J. Va’vra,⁶⁸ N. van Bakel,⁶⁸ A. P. Wagner,⁶⁸ M. Weaver,⁶⁸ W. J. Wisniewski,⁶⁸ M. Wittgen,⁶⁸ D. H. Wright,⁶⁸ A. K. Yarritu,⁶⁸ K. Yi,⁶⁸ C. C. Young,⁶⁸ P. R. Burchat,⁶⁹ A. J. Edwards,⁶⁹ S. A. Majewski,⁶⁹ B. A. Petersen,⁶⁹ L. Wilden,⁶⁹ S. Ahmed,⁷⁰ M. S. Alam,⁷⁰ R. Bula,⁷⁰ J. A. Ernst,⁷⁰ V. Jain,⁷⁰ B. Pan,⁷⁰ M. A. Saeed,⁷⁰ F. R. Wappler,⁷⁰ S. B. Zain,⁷⁰ W. Bugg,⁷¹ M. Krishnamurthy,⁷¹ S. M. Spanier,⁷¹ R. Eckmann,⁷² J. L. Ritchie,⁷² A. M. Ruland,⁷² C. J. Schilling,⁷² R. F. Schwitters,⁷² J. M. Izen,⁷³ X. C. Lou,⁷³ S. Ye,⁷³ F. Bianchi,⁷⁴ F. Gallo,⁷⁴ D. Gamba,⁷⁴ M. Pelliccioni,⁷⁴ M. Bomben,⁷⁵ L. Bosisio,⁷⁵ C. Cartaro,⁷⁵ F. Cossutti,⁷⁵ G. Della Ricca,⁷⁵ L. Lanceri,⁷⁵ L. Vitale,⁷⁵ V. Azzolini,⁷⁶ N. Lopez-March,⁷⁶ F. Martinez-Vidal,⁷⁶ D. A. Milanes,⁷⁶ A. Oyanguren,⁷⁶ J. Albert,⁷⁷ Sw. Banerjee,⁷⁷ B. Bhuyan,⁷⁷ K. Hamano,⁷⁷ R. Kowalewski,⁷⁷ I. M. Nugent,⁷⁷ J. M. Roney,⁷⁷ R. J. Sobie,⁷⁷ J. J. Back,⁷⁸ P. F. Harrison,⁷⁸ T. E. Latham,⁷⁸ G. B. Mohanty,⁷⁸ M. Pappagallo,^{78,§} H. R. Band,⁷⁹ X. Chen,⁷⁹ S. Dasu,⁷⁹ K. T. Flood,⁷⁹ J. J. Hollar,⁷⁹ P. E. Kutter,⁷⁹ Y. Pan,⁷⁹ M. Pierini,⁷⁹ R. Prepost,⁷⁹ S. L. Wu,⁷⁹ Z. Yu,⁷⁹ and H. Neal⁸⁰

(The BABAR Collaboration)

¹Laboratoire de Physique des Particules, IN2P3/CNRS et Université de Savoie, F-74941 Annecy-Le-Vieux, France

²Universitat de Barcelona, Facultat de Física, Departament ECM, E-08028 Barcelona, Spain

³Università di Bari, Dipartimento di Fisica and INFN, I-70126 Bari, Italy

⁴University of Bergen, Institute of Physics, N-5007 Bergen, Norway

⁵Lawrence Berkeley National Laboratory and University of California, Berkeley, California 94720, USA

⁶University of Birmingham, Birmingham, B15 2TT, United Kingdom

⁷Ruhr Universität Bochum, Institut für Experimentalphysik 1, D-44780 Bochum, Germany

⁸University of Bristol, Bristol BS8 1TL, United Kingdom

⁹University of British Columbia, Vancouver, British Columbia, Canada V6T 1Z1

¹⁰Brunel University, Uxbridge, Middlesex UB8 3PH, United Kingdom

¹¹Budker Institute of Nuclear Physics, Novosibirsk 630090, Russia

¹²University of California at Irvine, Irvine, California 92697, USA

¹³University of California at Los Angeles, Los Angeles, California 90024, USA

¹⁴University of California at Riverside, Riverside, California 92521, USA

¹⁵University of California at San Diego, La Jolla, California 92093, USA

¹⁶University of California at Santa Barbara, Santa Barbara, California 93106, USA

¹⁷University of California at Santa Cruz, Institute for Particle Physics, Santa Cruz, California 95064, USA

¹⁸California Institute of Technology, Pasadena, California 91125, USA

¹⁹University of Cincinnati, Cincinnati, Ohio 45221, USA

²⁰University of Colorado, Boulder, Colorado 80309, USA

²¹Colorado State University, Fort Collins, Colorado 80523, USA

²²Universität Dortmund, Institut für Physik, D-44221 Dortmund, Germany

²³Technische Universität Dresden, Institut für Kern- und Teilchenphysik, D-01062 Dresden, Germany

²⁴Laboratoire Leprince-Ringuet, CNRS/IN2P3, Ecole Polytechnique, F-91128 Palaiseau, France

²⁵University of Edinburgh, Edinburgh EH9 3JZ, United Kingdom

- ²⁶ *Università di Ferrara, Dipartimento di Fisica and INFN, I-44100 Ferrara, Italy*
²⁷ *Laboratori Nazionali di Frascati dell'INFN, I-00044 Frascati, Italy*
²⁸ *Università di Genova, Dipartimento di Fisica and INFN, I-16146 Genova, Italy*
²⁹ *Harvard University, Cambridge, Massachusetts 02138, USA*
³⁰ *Universität Heidelberg, Physikalisches Institut, Philosophenweg 12, D-69120 Heidelberg, Germany*
³¹ *Imperial College London, London, SW7 2AZ, United Kingdom*
³² *University of Iowa, Iowa City, Iowa 52242, USA*
³³ *Iowa State University, Ames, Iowa 50011-3160, USA*
³⁴ *Johns Hopkins University, Baltimore, Maryland 21218, USA*
³⁵ *Universität Karlsruhe, Institut für Experimentelle Kernphysik, D-76021 Karlsruhe, Germany*
³⁶ *Laboratoire de l'Accélérateur Linéaire, IN2P3/CNRS et Université Paris-Sud 11, Centre Scientifique d'Orsay, B. P. 34, F-91898 ORSAY Cedex, France*
³⁷ *Lawrence Livermore National Laboratory, Livermore, California 94550, USA*
³⁸ *University of Liverpool, Liverpool L69 7ZE, United Kingdom*
³⁹ *Queen Mary, University of London, E1 4NS, United Kingdom*
⁴⁰ *University of London, Royal Holloway and Bedford New College, Egham, Surrey TW20 0EX, United Kingdom*
⁴¹ *University of Louisville, Louisville, Kentucky 40292, USA*
⁴² *University of Manchester, Manchester M13 9PL, United Kingdom*
⁴³ *University of Maryland, College Park, Maryland 20742, USA*
⁴⁴ *University of Massachusetts, Amherst, Massachusetts 01003, USA*
⁴⁵ *Massachusetts Institute of Technology, Laboratory for Nuclear Science, Cambridge, Massachusetts 02139, USA*
⁴⁶ *McGill University, Montréal, Québec, Canada H3A 2T8*
⁴⁷ *Università di Milano, Dipartimento di Fisica and INFN, I-20133 Milano, Italy*
⁴⁸ *University of Mississippi, University, Mississippi 38677, USA*
⁴⁹ *Université de Montréal, Physique des Particules, Montréal, Québec, Canada H3C 3J7*
⁵⁰ *Mount Holyoke College, South Hadley, Massachusetts 01075, USA*
⁵¹ *Università di Napoli Federico II, Dipartimento di Scienze Fisiche and INFN, I-80126, Napoli, Italy*
⁵² *NIKHEF, National Institute for Nuclear Physics and High Energy Physics, NL-1009 DB Amsterdam, The Netherlands*
⁵³ *University of Notre Dame, Notre Dame, Indiana 46556, USA*
⁵⁴ *Ohio State University, Columbus, Ohio 43210, USA*
⁵⁵ *University of Oregon, Eugene, Oregon 97403, USA*
⁵⁶ *Università di Padova, Dipartimento di Fisica and INFN, I-35131 Padova, Italy*
⁵⁷ *Laboratoire de Physique Nucléaire et de Hautes Energies, IN2P3/CNRS, Université Pierre et Marie Curie-Paris6, Université Denis Diderot-Paris7, F-75252 Paris, France*
⁵⁸ *University of Pennsylvania, Philadelphia, Pennsylvania 19104, USA*
⁵⁹ *Università di Perugia, Dipartimento di Fisica and INFN, I-06100 Perugia, Italy*
⁶⁰ *Università di Pisa, Dipartimento di Fisica, Scuola Normale Superiore and INFN, I-56127 Pisa, Italy*
⁶¹ *Prairie View A&M University, Prairie View, Texas 77446, USA*
⁶² *Princeton University, Princeton, New Jersey 08544, USA*
⁶³ *Università di Roma La Sapienza, Dipartimento di Fisica and INFN, I-00185 Roma, Italy*
⁶⁴ *Universität Rostock, D-18051 Rostock, Germany*
⁶⁵ *Rutherford Appleton Laboratory, Chilton, Didcot, Oxon, OX11 0QX, United Kingdom*
⁶⁶ *DSM/Dapnia, CEA/Saclay, F-91191 Gif-sur-Yvette, France*
⁶⁷ *University of South Carolina, Columbia, South Carolina 29208, USA*
⁶⁸ *Stanford Linear Accelerator Center, Stanford, California 94309, USA*
⁶⁹ *Stanford University, Stanford, California 94305-4060, USA*
⁷⁰ *State University of New York, Albany, New York 12222, USA*
⁷¹ *University of Tennessee, Knoxville, Tennessee 37996, USA*
⁷² *University of Texas at Austin, Austin, Texas 78712, USA*
⁷³ *University of Texas at Dallas, Richardson, Texas 75083, USA*
⁷⁴ *Università di Torino, Dipartimento di Fisica Sperimentale and INFN, I-10125 Torino, Italy*
⁷⁵ *Università di Trieste, Dipartimento di Fisica and INFN, I-34127 Trieste, Italy*
⁷⁶ *IFIC, Universitat de Valencia-CSIC, E-46071 Valencia, Spain*
⁷⁷ *University of Victoria, Victoria, British Columbia, Canada V8W 3P6*
⁷⁸ *Department of Physics, University of Warwick, Coventry CV4 7AL, United Kingdom*
⁷⁹ *University of Wisconsin, Madison, Wisconsin 53706, USA*
⁸⁰ *Yale University, New Haven, Connecticut 06511, USA*

(Dated: September 14, 2018)

We determine the relative branching fractions of semileptonic B decays to charmed final states. The measurement is performed on the recoil from a fully reconstructed B meson in a sample of 362 million $B\bar{B}$ pairs collected at the $\Upsilon(4S)$ resonance with the BABAR detector. A simultaneous fit to a set of discriminating variables is performed on a sample of $\bar{B} \rightarrow DX\ell^-\bar{\nu}_\ell$ decays to determine

the contributions from the different channels. We measure $\Gamma(B^- \rightarrow D\ell^- \bar{\nu}_\ell)/\Gamma(B^- \rightarrow DX\ell^- \bar{\nu}_\ell) = 0.227 \pm 0.014 \pm 0.016$, $\Gamma(B^- \rightarrow D^*\ell^- \bar{\nu}_\ell)/\Gamma(B^- \rightarrow DX\ell^- \bar{\nu}_\ell) = 0.582 \pm 0.018 \pm 0.030$ and $\Gamma(B^- \rightarrow D^{**}\ell^- \bar{\nu}_\ell)/\Gamma(B^- \rightarrow DX\ell^- \bar{\nu}_\ell) = 0.191 \pm 0.013 \pm 0.019$ for the charged B sample, and $\Gamma(\overline{B}^0 \rightarrow D\ell^- \bar{\nu}_\ell)/\Gamma(\overline{B}^0 \rightarrow DX\ell^- \bar{\nu}_\ell) = 0.215 \pm 0.016 \pm 0.013$, $\Gamma(\overline{B}^0 \rightarrow D^*\ell^- \bar{\nu}_\ell)/\Gamma(\overline{B}^0 \rightarrow DX\ell^- \bar{\nu}_\ell) = 0.537 \pm 0.031 \pm 0.036$ and $\Gamma(\overline{B}^0 \rightarrow D^{**}\ell^- \bar{\nu}_\ell)/\Gamma(\overline{B}^0 \rightarrow DX\ell^- \bar{\nu}_\ell) = 0.248 \pm 0.032 \pm 0.030$ for the neutral B sample, where uncertainties are statistical and systematic, respectively.

PACS numbers: 13.20He,12.38.Qk,14.40Nd

The determination of exclusive branching fractions of $\overline{B} \rightarrow X_c\ell^- \bar{\nu}_\ell$ decays is an essential part of the B -factory program to understand the dynamics of b -quark semileptonic decays and to determine the relevant Cabibbo-Kobayashi-Maskawa matrix elements [1]. The mass of the hadronic system X_c , recoiling against the leptonic pair, is a crucial observable both in the extraction of $|V_{cb}|$, in exclusive semileptonic decays, and in isolating $\overline{B} \rightarrow X_u\ell^- \bar{\nu}_\ell$ decays to determine $|V_{ub}|$. It is also needed for the measurement of heavy quark masses and other non-perturbative OPE (Operator Product Expansion) parameters from the distribution of spectral moments. This mass spectrum can be better understood by a study of the yields of the different D meson states in semileptonic decays. Current measurements [2, 3, 4, 5] show a possible discrepancy between the sum of exclusive rates and the inclusive semileptonic decay width [6]. While $\overline{B} \rightarrow D\ell^- \bar{\nu}_\ell$ and $\overline{B} \rightarrow D^*\ell^- \bar{\nu}_\ell$ decays account for about 70% of this total, the contribution of other states, including resonant and non-resonant $D^{(*)}\pi$ decays, is not yet well measured and is a possible explanation of this discrepancy.

In this paper, we present a novel technique to extract the exclusive relative branching fractions for $\overline{B} \rightarrow D\ell^- \bar{\nu}_\ell$, $\overline{B} \rightarrow D^*\ell^- \bar{\nu}_\ell$ and $\overline{B} \rightarrow D^{**}\ell^- \bar{\nu}_\ell$, with $\ell = e, \mu$ [7], from an inclusive sample of $\overline{B} \rightarrow DX\ell^- \bar{\nu}_\ell$ events, where X can be either nothing or any particle(s) from a semileptonic B decay into a higher mass charm state, or a non-resonant state. We denote by D^{**} any hadronic final state, containing a charm meson, with total mass above that of the D^* state, thereby including both D_J excited mesons and $D^{(*)}+n\pi$ non-resonant states. This technique ensures sensitivity to all hadronic final states containing a D meson, thus helping us to understand the role of excited D states in saturating the inclusive semileptonic rate.

This analysis is based on data collected with the *BABAR* detector [8] at the PEP-II asymmetric-energy e^+e^- storage rings. The data correspond to an integrated luminosity of 339.4 fb^{-1} recorded at the $\Upsilon(4S)$ resonance, or, equivalently, about 362 million $B\overline{B}$ pairs. A detailed GEANT4-based Monte Carlo (MC) simulation [9] of $B\overline{B}$

and continuum $e^+e^- \rightarrow f\bar{f}$ ($f = u, d, s, c, \tau$) events has been used to study the detector response and its acceptance. The simulation models $\overline{B} \rightarrow D^*\ell^- \bar{\nu}_\ell$ decays using HQET-based calculations [10], $\overline{B} \rightarrow D\ell^- \bar{\nu}_\ell$ and $\overline{B} \rightarrow D^{**}(\rightarrow D^{(*)}\pi)\ell^- \bar{\nu}_\ell$ decays using the ISGW2 model [11], and $\overline{B} \rightarrow D^{(*)}\pi\ell^- \bar{\nu}_\ell$ decays using the Goity-Roberts model [12].

We select signal B -meson decays in events containing a fully reconstructed B meson (B_{tag}), which allows us to constrain the kinematics, to reduce the combinatorial background and to determine the charge and flavor of the signal B . We choose a set of three largely uncorrelated variables to discriminate between the different semileptonic decay modes in the reconstructed $\overline{B} \rightarrow DX\ell^- \bar{\nu}_\ell$ sample. These are: i) the lepton momentum in the center-of-mass (CM) frame, $|\vec{p}_\ell|$; ii) the missing mass squared reconstructed with respect to the $D\ell$ system, which corresponds to the mass of the $X\bar{\nu}_\ell$ system, $m_{miss,D}^2 = (p_\ell - p_{B_{tag}} - p_D - p_\ell)^2$, where p_i is the four momentum in the CM frame of the reconstructed state i ; and iii) the number of reconstructed charged tracks in addition to those used for reconstructing the $D\ell$ system and the B_{tag} , N_{trks} . In order to reduce the sensitivity to the modeling of the decays to the different charm states, the shapes of these variables are extracted from data, using exclusive samples highly enriched in the relevant decay modes. The relative D , D^* and D^{**} contributions are then determined by a multiparameter fit to the inclusive sample.

We select semileptonic B decays that contain one fully reconstructed D meson and that recoil against a fully reconstructed B_{tag} decaying hadronically. To obtain a high reconstruction efficiency, the analysis exploits the presence of two charmed mesons in the final state: one used for the exclusive reconstruction of the B_{tag} , and another in the semileptonic B decay.

The event reconstruction starts from the semileptonic B decay, selecting a charm meson and a lepton with momentum in the CM frame higher than $0.6 \text{ GeV}/c$ and the correct charge-flavor correlation. Candidate D^0 mesons are reconstructed in the $K^-\pi^+$, $K^-\pi^+\pi^0$, $K^-\pi^+\pi^+\pi^-$, $K_S^0\pi^+\pi^-$, $K_S^0\pi^+\pi^-\pi^0$, $K_S^0\pi^0$, K^+K^- , $\pi^+\pi^-$, and $K_S^0K_S^0$ channels, and D^+ mesons in the $K^-\pi^+\pi^+$, $K^-\pi^+\pi^+\pi^0$, $K_S^0\pi^+$, $K_S^0\pi^+\pi^0$, $K^+K^-\pi^+$, $K_S^0K^+$, and $K_S^0\pi^+\pi^+\pi^-$ channels. In events with multiple candidates, the candidate with the largest D - ℓ vertex fit probability is selected. We then select a fully reconstructed B_{tag} meson candidate. We reconstruct B_{tag} decays of the type $\overline{B} \rightarrow DY$, where Y represents a collection of hadrons with a total

*Deceased

†Also with Università di Perugia, Dipartimento di Fisica, Perugia, Italy

‡Also with Università della Basilicata, Potenza, Italy

§Also with IPPP, Physics Department, Durham University, Durham DH1 3LE, United Kingdom

charge of ± 1 , composed of $n_1\pi^\pm + n_2K^\pm + n_3K_S^0 + n_4\pi^0$, where $n_1 + n_2 \leq 5$, $n_3 \leq 2$, and $n_4 \leq 2$. Using $D^0(D^+)$ and $D^{*0}(D^{*+})$ as seeds for $B^-(\overline{B}^0)$ decays, we reconstruct about 1000 different decay chains.

The kinematic consistency of a B_{tag} candidate with a B -meson decay is checked using two variables: the beam-energy substituted mass $m_{ES} = \sqrt{s/4 - |\vec{p}_B|^2}$, and the energy difference $\Delta E = E_B - \sqrt{s}/2$. Here \sqrt{s} refers to the total CM energy, and $|\vec{p}_B|$ and E_B denote the momentum and energy of the B_{tag} candidate in the CM frame. For correctly identified B_{tag} decays, the m_{ES} distribution peaks at the B meson mass, while ΔE is consistent with zero. We select the B_{tag} candidate that has no daughter particles in common with the charm meson and the lepton from the semileptonic B decay, m_{ES} within the signal region defined as $5.27 \text{ GeV}/c^2 < m_{ES} < 5.29 \text{ GeV}/c^2$, and the smallest $|\Delta E|$ value. Mixing effects in the \overline{B}^0 sample are accounted for as described in [13].

The $\overline{B} \rightarrow DX\ell^-\bar{\nu}_\ell$ decays are identified by relatively loose selection criteria. We require the reconstructed ground-state charm meson invariant mass M_{D^0} (M_{D^+}) to be in the range from 1.850 (1.853) GeV/c^2 to 1.880 (1.883) GeV/c^2 and the cosine of the angle between the directions of the D candidate and the lepton in the CM frame to be less than zero, to reduce background from non- B semileptonic decays.

After these selection criteria, the sample contains leptons from prompt B decays, as well as cascade B decays, in which the lepton does not come directly from the B . There are also background sources of leptons, such as photon conversions and Dalitz π^0 decays, combinatorial $B\overline{B}$ background and continuum events, that need to be subtracted. The contamination from cascade B decays, about 15.1 (17.8)% of the total $B^-(\overline{B}^0)$ sample, is subtracted using the simulated MC distributions for these backgrounds. These events are reweighted to account for differences among the branching fractions used in our MC simulation and the latest experimental measurements [14]. The photon conversion and π^0 Dalitz decay backgrounds (less than 0.8% of the total electron sample) are removed using a dedicated algorithm, which performs the reconstruction of vertices between tracks of opposite charges whose invariant mass is compatible with a photon conversion or a π^0 Dalitz decay. The contributions of combinatorial and continuum B_{tag} backgrounds are estimated from the m_{ES} sideband region $5.21 \text{ GeV}/c^2 < m_{ES} < 5.26 \text{ GeV}/c^2$. The m_{ES} distribution is fitted by the sum of a Gaussian function joined to an exponential tail [15] for the signal and an empirical phase-space threshold function [16] for the background. Cross-feed effects, i.e. $B_{tag}^-(\overline{B}_{tag}^0)$ candidates erroneously reconstructed as a neutral (charged) B , are corrected using MC simulations. We estimate the fraction of cross-feed events in the reconstructed $B^-(\overline{B}^0)$ sample to be 6.8% (8.1%). A total of 6396 ± 251 (2981 ± 122) events are selected, with an estimated purity in $B^-(\overline{B}^0) \rightarrow DX\ell^-\bar{\nu}_\ell$ of 72% (73.8%).

Exclusive samples enriched in $D\ell^-\bar{\nu}_\ell$, $D^*\ell^-\bar{\nu}_\ell$ and

TABLE I: Invariant mass ranges for D^{*0} and D^{*+} selection.

Mode	Selection Criteria
$D^{*0} \rightarrow D^0\pi^0$	$0.139 < M(D^{*0}) - M(D^0) < 0.145 \text{ GeV}/c^2$
$D^{*0} \rightarrow D^0\gamma$	$0.133 < M(D^{*0}) - M(D^0) < 0.151 \text{ GeV}/c^2$
$D^{*+} \rightarrow D^0\pi^+$	$0.141 < M(D^{*+}) - M(D^0) < 0.149 \text{ GeV}/c^2$
$D^{*+} \rightarrow D^+\pi^0$	$0.138 < M(D^{*+}) - M(D^+) < 0.143 \text{ GeV}/c^2$

$D^{(*)}\pi\ell^-\bar{\nu}_\ell$ are then selected. Contributions from other semileptonic B decays into charm final states, where one or more particles from a higher mass charm state are missing (feed-down) or random particles are erroneously associated with the charm candidate (feed-up) are removed. This is done by selecting signal regions in the missing mass squared distributions $m_{miss,D^{(*,**)}}^2 = (p_\ell - p_{B_{tag}} - p_{D^{(*,**)}} - p_\ell)^2$ corresponding to the exclusive decay being reconstructed. The selection criteria are chosen to maximize the sample purity. We select D^{*+} and D^{*0} candidates by requiring the invariant mass difference between the D^* and the D to satisfy the selection criteria in Table I.

The $B^- \rightarrow D^{*0}\ell^-\bar{\nu}_\ell$ and $\overline{B}^0 \rightarrow D^{*+}\ell^-\bar{\nu}_\ell$ decays are selected by requiring the missing mass squared $m_{miss,D^{*0}}^2$ to be between $-0.35 \text{ GeV}^2/c^4$ and $0.5 \text{ GeV}^2/c^4$ and $|m_{miss,D^{*+}}^2|$ to be smaller than $0.55 \text{ GeV}^2/c^4$, respectively. Feed-down events from decays to D^{**} states are removed by requiring $m_{miss,D^{**0}}^2$ and $m_{miss,D^{**+}}^2$ to be incompatible with zero. The $B^- \rightarrow D^0\ell^-\bar{\nu}_\ell$ and $\overline{B}^0 \rightarrow D^+\ell^-\bar{\nu}_\ell$ decays are selected by removing feed-down events from D^* and D^{**} states. Similar selection criteria are applied for $B^- \rightarrow D^{*0}\ell^-\bar{\nu}_\ell$ decays, with $D^{*0} \rightarrow D^{(*)+}\pi^-$, and $\overline{B}^0 \rightarrow D^{*+}\ell^-\bar{\nu}_\ell$ decays, with $D^{*+} \rightarrow D^{(*)0}\pi^+$.

The probability density functions (PDFs) of the discriminating variables, $|\vec{p}_\ell|$, $m_{miss,D}^2$ and N_{trks} are determined using the exclusive samples. In order to test for possible selection biases in the PDF shapes, the inclusive distributions for MC samples of $\overline{B} \rightarrow D\ell^-\bar{\nu}_\ell$, $D^*\ell^-\bar{\nu}_\ell$ and $D^{(*)}\pi\ell^-\bar{\nu}_\ell$ events have been compared to those obtained after the exclusive event selection. Good agreement is found after accounting for the residual background from feed-down and feed-up from other modes. The PDFs are parameterized as sums of analytic functions, such as Gaussians and polynomials, with the exception of N_{trks} which is described using histograms.

The relative fractions of D , D^* and D^{**} decays in the selected inclusive sample of $\overline{B} \rightarrow DX\ell^-\bar{\nu}_\ell$ events are obtained by a simultaneous χ^2 fit to the inclusive and exclusive $|\vec{p}_\ell|$, $m_{miss,D}^2$ and N_{trks} distributions. The relative fractions are floated, constraining their sum to be one, together with the parameters of the functions describing the shapes of the discriminating variables. This results in a 35-parameter fit, which ensures that statistical correlations between the different samples are properly taken into account and the uncertainties in the exclusive shapes, obtained from samples of significantly

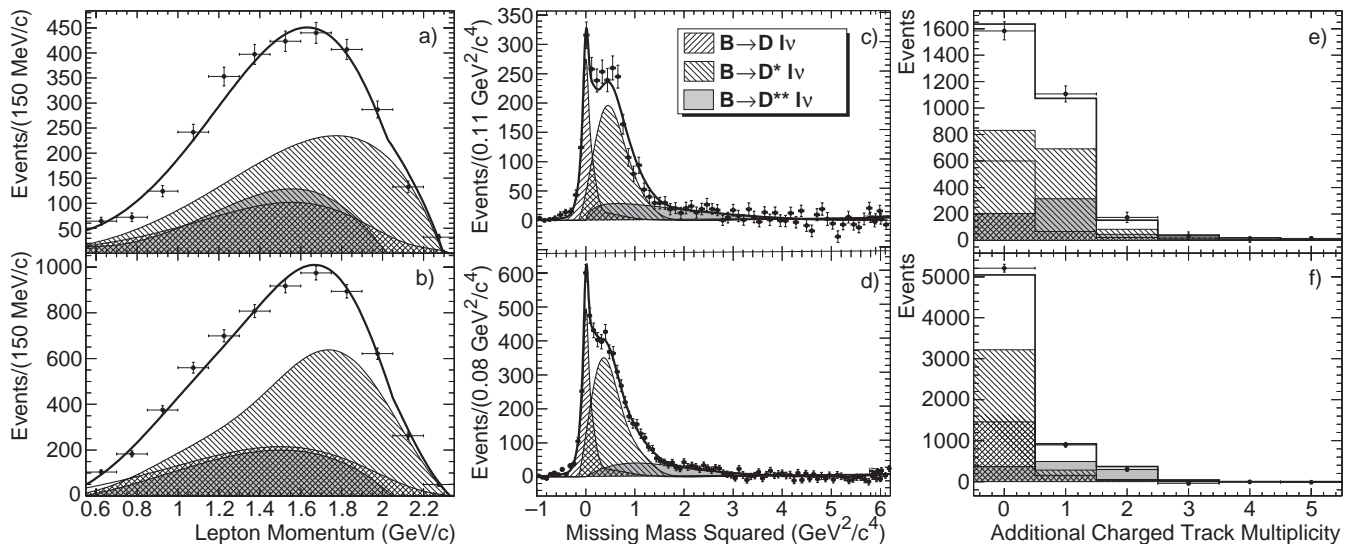


FIG. 1: Fitted $|\vec{p}_\ell|$ (a,b), $m_{miss,D}^2$ (c,d), and N_{trks} (e,f) distributions for $\overline{B}^0 \rightarrow DX\ell^-\bar{\nu}_\ell$ (top) and $B^- \rightarrow DX\ell^-\bar{\nu}_\ell$ (bottom). The PDFs corresponding to the different exclusive components are superposed with different filling styles.

smaller size compared to that of the inclusive sample, are correctly propagated into the statistical uncertainties on the D , D^* and D^{**} relative fractions. Since this analysis does not reconstruct D^{**} states with neutral pions, the N_{trks} distribution for states with the same charged-track multiplicity is used to model these decays: e.g. the $B^- \rightarrow D^{*0}\ell^-\bar{\nu}_\ell$ N_{trks} distribution is used for modeling $D^{*0}(\rightarrow D^{*0}\pi^0)\ell^-\bar{\nu}_\ell$ decays. For the modes involving a soft charged pion, such as $\overline{B}^0 \rightarrow D^{*+}\ell^-\bar{\nu}_\ell$, the MC prediction for the additional charged-track multiplicity distribution is used to account for inefficiencies in the reconstruction of the low-momentum particle. MC studies show that the PDFs for the $\overline{B} \rightarrow D^{**}\ell^-\bar{\nu}_\ell$ component, obtained by the exclusive reconstruction of $\overline{B} \rightarrow D^{(*)}\pi\ell^-\bar{\nu}_\ell$ decays, can also be used to parameterize $\overline{B} \rightarrow D^{(*)}n\pi\ell^-\bar{\nu}_\ell$ decays in the inclusive $\overline{B} \rightarrow DX\ell^-\bar{\nu}_\ell$ sample. The fit also accounts for feed-down and feed-up decays in the exclusive shapes, fixing the relative contributions to the predictions from the simulation. The fit performance has been extensively tested using simulated samples with varying fractions of the different decay modes. These tests show that the procedure adopted in this analysis is able to extract the decay fractions without any significant bias. The statistical uncertainty obtained by the fit reproduces the scatter of the results from independent samples, where the bin contents of the distributions have been fluctuated according to their statistical uncertainty. The fit results for the $\overline{B}^0 \rightarrow DX\ell^-\bar{\nu}_\ell$ and $B^- \rightarrow DX\ell^-\bar{\nu}_\ell$ distributions of the three variables $|\vec{p}_\ell|$, $m_{miss,D}^2$ and N_{trks} are shown in Fig. 1. The fit has a χ^2 value of 200 for 212 degrees of freedom for the B^- sample and 204 for 168 degrees of freedom for the \overline{B}^0 sample.

Several stability checks have been performed. First the sample has been split into sub-samples based on the lepton flavor and the run period and the fit has been

repeated for each one of them. Results are consistent within the statistical uncertainties. As another check, the $\overline{B} \rightarrow D\ell^-\bar{\nu}_\ell$ and $\overline{B} \rightarrow D^*\ell^-\bar{\nu}_\ell$ branching fractions have been determined by a binned likelihood fit to the $m_{miss,D}^2$ and m_{miss,D^*}^2 distributions respectively, where simulated events are used to model the shape of the missing mass squared variables for the D , D^* and D^{**} exclusive decays and the combinatorial and continuum background. The results are in good agreement with the relative branching fractions obtained from the fit to the inclusive $\overline{B} \rightarrow DX\ell^-\bar{\nu}_\ell$ sample, once we normalize them to the total semileptonic B branching fraction.

Different sources of systematic uncertainties have been investigated and are given in Table II. The first source is due to detector effects, where the size of the uncertainties in the detector response are determined from data control samples. Uncertainties related to the reconstruction of charged tracks are determined by evaluating the fit stability using different track selection criteria and by a MC study in which we vary the track multiplicity according to the tracking efficiency uncertainty. The systematic error due to the reconstruction of neutral particles is studied by varying the simulated calorimeter resolution and efficiency. The systematic uncertainty from lepton identification is estimated by varying the tagging efficiency by 2% (3%) for electrons (muons) and the misidentification probability by 15%.

The second main source of systematic uncertainty is related to the selection of the inclusive sample. A major contribution is due to background processes, where the estimated systematic error is dominated by the uncertainty on the weighting factors used to subtract B cascade decays. The uncertainty in the subtraction of the background from the fully reconstructed B_{tag} decays is evaluated from the differences in the shapes of this back-

TABLE II: Relative errors (%) in the determination of $\Gamma(\overline{B} \rightarrow D^{(*,**)}\ell^-\bar{\nu}_\ell)/\Gamma(\overline{B} \rightarrow DX\ell^-\bar{\nu}_\ell)$.

	$B^-/\overline{B}^0 \rightarrow D\ell^-\bar{\nu}_\ell$	$B^-/\overline{B}^0 \rightarrow D^*\ell^-\bar{\nu}_\ell$	$B^-/\overline{B}^0 \rightarrow D^{**}\ell^-\bar{\nu}_\ell$
Tracking reconstruction	3.54/2.36	1.3/0.3	4.63/3.14
Neutral reconstruction	0.38/0.3	0.39/0.31	0.41/0.34
Lepton identification	3.46/3.24	3.71/3.57	3.51/3.3
$\overline{B} \rightarrow DX\ell^-\bar{\nu}_\ell$ Backgrounds	0.48/0.78	1.69/4.13	5.11/7.19
$\overline{B} \rightarrow DX\ell^-\bar{\nu}_\ell$ Reconstruction efficiency	2.35/3.52	1.53/2.6	3.37/6.43
$\overline{B} \rightarrow DX\ell^-\bar{\nu}_\ell$ Cross-feed corrections	0.23/0.46	0.13/0.56	0.71/0.97
$\overline{B} \rightarrow D^{(*,**)}\ell^-\bar{\nu}_\ell$ Backgrounds	1.81/1.46	1.04/1.41	1.87/2.26
$\overline{B} \rightarrow D^{(*,**)}\ell^-\bar{\nu}_\ell$ Feed-down and feed-up corrections	1.99/1.49	1.31/1.34	1.84/2.01
$\overline{B} \rightarrow D^{(*,**)}\ell^-\bar{\nu}_\ell$ Cross feed corrections	0.74/0.62	0.1/0.23	1.33/0.74
$ \vec{p}_\ell $ and m_{miss}^2 PDFs	3.27/1.68	1.06/1.81	1.64/4.8
N_{trks} PDF	0.38/0.9	0.91/0.2	3.68/0.86
$\overline{B} \rightarrow D^{(*)}n\pi\ell^-\bar{\nu}_\ell$	0.9/0.73	1.1/0.89	0.89/0.72
Total Syst.	7.06/6.19	5.18/6.71	9.88/12.2

ground in the sideband and in the signal region using MC predictions. The systematic error due to the uncertainty in the amount of flavor cross-feed is computed by varying its fraction by a conservative 30%. The corresponding systematic uncertainties are evaluated for the exclusive samples. The analysis, relying on decay classification in an inclusive sample, is not sensitive, at first order, to reconstruction efficiencies. There remains an uncertainty arising from possible differences in efficiencies for the various channels, which is estimated from simulation.

Systematic uncertainties due to the PDFs are estimated by replacing the shapes extracted from the exclusive samples with those predicted by our simulation and repeating the fit. Additionally the uncertainty in the relative $D^{**0} \rightarrow D^{(*)}\pi^-$ to $D^{**0} \rightarrow D^{(*)0}\pi^0$ reconstruction efficiency is accounted for by varying the N_{trks} distribution for the D^{**0} component.

Systematic effects due to $\overline{B} \rightarrow D^{(*)}n\pi\ell^-\bar{\nu}_\ell$ events not well parameterized by the $\overline{B} \rightarrow D^{**}\ell^-\bar{\nu}_\ell$ PDFs are estimated by repeating the fit with an additional component for these events. The corresponding PDFs are built from a sample of simulated $\overline{B} \rightarrow D^{(*)}\pi\pi\ell^-\bar{\nu}_\ell$ events. The observed difference in the fit results is taken as an additional systematic error.

TABLE III: Fitted ratios of branching fractions with statistical and systematic uncertainties.

Ratio	B^- (%)	\overline{B}^0 (%)
$\frac{\Gamma(\overline{B} \rightarrow D\ell^-\bar{\nu}_\ell)}{\Gamma(\overline{B} \rightarrow DX\ell^-\bar{\nu}_\ell)}$	$22.7 \pm 1.4 \pm 1.6$	$21.5 \pm 1.6 \pm 1.3$
$\frac{\Gamma(\overline{B} \rightarrow D^*\ell^-\bar{\nu}_\ell)}{\Gamma(\overline{B} \rightarrow DX\ell^-\bar{\nu}_\ell)}$	$58.2 \pm 1.8 \pm 3.0$	$53.7 \pm 3.1 \pm 3.6$
$\frac{\Gamma(\overline{B} \rightarrow D^{**}\ell^-\bar{\nu}_\ell)}{\Gamma(\overline{B} \rightarrow DX\ell^-\bar{\nu}_\ell)}$	$19.1 \pm 1.3 \pm 1.9$	$24.8 \pm 3.2 \pm 3.0$

In summary, the relative branching fractions for the $B^- \rightarrow D^0, D^{*0}, D^{**0}\ell^-\bar{\nu}_\ell$ and $\overline{B}^0 \rightarrow D^+, D^{*+}, D^{**+}\ell^-\bar{\nu}_\ell$ decays have been determined by a multiparameter fit to three discriminating variables in an inclusive sample of $\overline{B} \rightarrow DX\ell^-\bar{\nu}_\ell$ events recoiling against a fully reconstructed B meson. The results are given in Table III. Apart from possible isospin violation effects, which are thought to be small, these three ratios are expected to be equal for B_u^- and \overline{B}_d^0 mesons. The results for charged and neutral B mesons are compatible within their uncorrelated uncertainties. Therefore the relative fractions have been averaged, accounting for correlated errors. The results are: $\Gamma(\overline{B} \rightarrow D\ell^-\bar{\nu}_\ell)/\Gamma(\overline{B} \rightarrow DX\ell^-\bar{\nu}_\ell) = 0.221 \pm 0.012$ (stat.) ± 0.006 (uncorr. syst.) ± 0.010 (corr. syst.), $\Gamma(\overline{B} \rightarrow D^*\ell^-\bar{\nu}_\ell)/\Gamma(\overline{B} \rightarrow DX\ell^-\bar{\nu}_\ell) = 0.572 \pm 0.017$ (stat.) ± 0.016 (uncorr. syst.) ± 0.022 (corr. syst.), $\Gamma(\overline{B} \rightarrow D^{**}\ell^-\bar{\nu}_\ell)/\Gamma(\overline{B} \rightarrow DX\ell^-\bar{\nu}_\ell) = 0.197 \pm 0.013$ (stat.) ± 0.013 (uncorr. syst.) ± 0.012 (corr. syst.), where the first uncertainty is statistical, the second the uncorrelated systematic and the third the correlated systematic error. The accuracy of these measurements is comparable to that of the current world average [6].

We are grateful for the excellent luminosity and machine conditions provided by our PEP-II colleagues, and for the substantial dedicated effort from the computing organizations that support BABAR. The collaborating institutions wish to thank SLAC for its support and kind hospitality. This work is supported by DOE and NSF (USA), NSERC (Canada), IHEP (China), CEA and CNRS-IN2P3 (France), BMBF and DFG (Germany), INFN (Italy), FOM (The Netherlands), NFR (Norway), MIST (Russia), MEC (Spain), and PPARC (United Kingdom). Individuals have received support from the Marie Curie EIF (European Union) and the A. P. Sloan Foundation.

-
- [1] M. Kobayashi and T. Maskawa, *Prog. Theor. Phys.* **49**, 652 (1973).
- [2] D. Skurowski *et al.* (ALEPH Collab.), *Z. Phys. C* **73**, 601 (1997).
- [3] P. Abreu *et al.* (DELPHI Collab.), *Phys. Lett. B* **475**, 407 (2000).
- [4] B. Aubert *et al.* (BABAR Collab.), *Phys. Rev. D* **71**, 051502 (2005).
- [5] D. Liventsev *et al.* (Belle Collab.), *Phys. Rev. D* **72**, 051109 (2005).
- [6] W. M. Yao *et al.* (Particle Data Group), *J. Phys. G* **33**, 1 (2006).
- [7] Charge conjugate states are always implied unless stated otherwise.
- [8] B. Aubert *et al.* (BABAR Collab.), *Nucl. Inst. Meth. A* **479**, 1 (2002).
- [9] S. Agostinelli *et al.*, *Nucl. Inst. Meth. A* **506**, 250 (2003).
- [10] J. Dubosq *et al.* (CLEO Collab.), *Phys. Rev. Lett.* **76**, 3898 (1996).
- [11] D. Scora and N. Isgur, *Phys. Rev. D* **52**, 2783 (1995). See also N. Isgur *et al.*, *Phys. Rev. D* **39**, 799 (1989).
- [12] L. Goity and W. Roberts, *Phys. Rev. D* **51**, 3459 (1995).
- [13] B. Aubert *et al.* (BABAR Collab.), *Phys. Rev. D* **69**, 111104 (2004).
- [14] B. Aubert *et al.* (BABAR Collab.), *Phys. Rev. D* **74**, 091105 (2006).
- [15] M. J. Oreglia, SLAC-236 (1980); J. E. Gaiser, SLAC-255 (1982); T. Skwarnicki, DESY F31-86-02 (1986).
- [16] H. Albrecht *et al.* (ARGUS Collab.), *Z. Phys. C* **48**, 543 (1990).